Journal of Medical Ultrasonics (2019) 46:113–122
https://doi.org/10.1007/s10396-018-0906-x

ORIGINAL ARTICLE

Three-dimensional sonographic minute structure analysis of fetal cerebellar vermis development and malformations: utilizing volume contrast imaging

Jing-xian Xie[1] · Jian-hong You[2] · Xiao-kang Chen[3] · Yi-ming Su[4] · Jin-rong Liu[5] · Shan-shan Su[6] · Min Hou[7] · Guo-rong Lv[8,9]

Received: 13 July 2018 / Accepted: 3 September 2018 / Published online: 5 October 2018

Abstract

Purpose To obtain three-dimensional ultrasonic (3D US) structural details and biometrics of the fetal cerebellar vermis and evaluate the value of developmental and malformation identification.

Methods The 3D US minute structure of the fetal cerebellar vermis in mid-sagittal view was detected in normal fetuses ($n=438$; 16–41 weeks). Biometric sizes were measured to establish the stage-specific norms and reproducibility analysis. Additionally, 28 fetuses with suspected abnormal posterior fossa contents were assessed to analyze the clinical value.

Results The minute structure of normal fetuses, including cerebellar vermis contours and the fastigial recess of the fourth ventricle, were visible around Week 19. The main lobules and fissures were apparent around Week 22, and all nine lobules, fissures, and the fourth ventricle were clearly displayed by Week 28. Cerebellar vermis biometric sizes (anterior–posterior length, cranio-caudal length, circumference, and surface area (SA)) grew in a linear fashion with high reliability, especially SA measurements (for intraclass, ICC 0.989, 95% CI (0.980–0.994); for interclass, ICC 0.992, 95% CI (0.984–0.996)). On the middle sagittal section of 3D US, the SA reduced at least 50% in the Dandy–Walker group with no recognizable cerebellar vermis structures showing. The SA in vermian hypoplasia malformation reduced during $\bar{x} - 2\mathrm{SD}$ to 50% with the primary/secondary fissures absent or partly absent and arborization of the lobules reduced. That would be an important diagnosis and antidiastole clue. Combined with minute structural observation, sonographic diagnoses were accurate in 88% of cases.

Conclusion Minute structures obtained by 3D US were clinically useful in the evaluation of cerebellar vermis development and cerebellar vermis malformations.

Keywords Three-dimensional ultrasonography · Fetus · Cerebellar vermis · Malformation · Minute structure

Jing-xian Xie and Jian-hong You equal contributors.

✉ Guo-rong Lv
lgr_feus@sina.com

[1] Department of Obstetrics and Gynecology, Xiamen Maternity and Child Health Care Hospital, Xiamen 361000, Fujian, People's Republic of China

[2] Department of Ultrasound, Zhongshan Hospital of Xiamen University, Xiamen 361000, Fujian, People's Republic of China

[3] Department of Ultrasound, Children's Hospital of Fudan University Xiamen Branch, Xiamen Children's Hospital, Xiamen 361000, Fujian, People's Republic of China

[4] Department of Ultrasound, The First Affiliated Hospital of Xiamen University, Xiamen 361000, Fujian, People's Republic of China

[5] Department of Ultrasound, Guangzhou Women and Children Medical Center, Guangzhou 510000, People's Republic of China

[6] Department of Ultrasound, The Second Clinical Medical College of Fujian Medical University, Quanzhou 362000, Fujian, People's Republic of China

[7] Department of Ultrasound, Affiliated Hospital of Hebei University, Baoding 071000, People's Republic of China

[8] Department of Clinical Medicine, Quanzhou Medical College, Quanzhou 362000, Fujian, People's Republic of China

[9] Quanzhou, People's Republic of China

Introduction

Evaluation of the subtle structure in the fetal posterior fossa is an important component of fetal anatomic pathology, generally regarded as the ''gold standard'' of cerebellar vermis diagnosis [1, 2]. Fetal posterior fossa anomalies such as Dandy–Walker syndrome and vermian dysgenesis range from benign asymptomatic conditions to severe mental retardation [3]. Reviewing the published literature, the discordance rates between prenatal findings and postnatal diagnosis (autopsy or radiologic imaging) were found to be as high as 32% to 100% [4, 5].

With improvements in prenatal diagnostic techniques, more attention has been given to imaging of fetal posterior fossa anomalies. Fetal posterior fossa abnormalities, particularly cerebellar vermis malformations, are extremely difficult to diagnose due to subtle anatomical differences [6]. Recently, new advances in prenatal imaging have allowed more detailed evaluation of posterior fossa contents, and several papers have reported the feasibility of hindbrain structure depiction and indirect signs for prenatal diagnosis of suspected cerebral malformations [2, 6–8]. In these reports, 2D ultrasound, three-dimensional ultrasonography (3D US), and MR imaging were the most commonly utilized methods for evaluation. Katorza et al. [2] compared the clinical usage of these three modalities and reported that all of them proved to be an excellent screening tool with high repeatability and consistency. Taking the advantages into consideration, ultrasound was available for antenatal measurements, as it was easy to follow-up subjects in a convenient, time-saving way with fewer contraindications.

3D US was reported to be extremely significant in prenatal evaluation of the fetal spleen, thyroid, and vermis, etc. [9, 10]. Compared to 2D ultrasound, 3D US did not limit fetal position, and the relevant order plane was easily reconstructed for offline analysis. The mid-sagittal plane is proposed as the most important plane to be investigated, because it enables visualization of the entire cerebellar structure (lobules, fourth ventricle, pons, and corpus callosum) and allows for the measurement of biometric sizes (antero-posterior length, cranio-caudal length, circumference, and surface area) of the cerebellar vermis. Coincidentally, the mid-sagittal view obtained by 3D US has been suggested as a valuable tool in the quantitative analysis of fetal cerebellar vermis development and malformation in both prenatal ultrasound and autopsy [11, 12].

At present, however, controversies over the classification of cerebellar vermis malformations are still prevalent, with no widely accepted diagnostic criterion for quantification as yet. In addition, due to the lack of an established approach and inadequate data in sonographic appearance and temporal changes between prenatal ultrasound and autopsy results, clinical usage has its limitation [4, 5, 9]. Hence, the main objectives of the present study were: (1) to obtain the minute morphological characteristics and quantitative biometric references of the fetal cerebellar vermis on the mid-sagittal plane at different gestational ages (GA) and (2) to evaluate whether the minute structure and norm on the mid-sagittal plane obtained by 3D US will be helpful to clinical diagnosis of cerebellar vermis malformations.

Materials and methods

Study site and device

This cross-sectional study was performed between September 2015 and December 2017 in the Ultrasound Department of Fujian Medical University. Approval for the study was obtained from the Ethics Committee, and informed consent was obtained from the participants prior to the study.

Examinations were performed with high-resolution equipment (4–8-MHz transabdominal transducers and a Voluson 730 expert system; General Electric Kretztechnik, Zipf, Austria).

Study population and design

Prior to the study, routine maternity ultrasound examinations were performed on all fetuses by transabdominal 3D US. A total of 438 fetuses (16–41 gestational weeks) with a normal cerebellar vermis structure were selected as controls. Inclusion criteria for the control group included the following items: singleton pregnancy, GA (confirmed by ultrasonic estimation of the crown-rump length early in the first trimester) based on the last menstrual period, and no identifiable malformations found during prenatal and postpartum routine sonographic examination. Cases that could not be imaged clearly with sonography were all excluded from our study. All prenatal diagnoses were confirmed with autopsy or detailed postnatal follow-up.

The best regression models to characterize the biometrics of the fetal vermis in relation to GA were identified by linear regression analysis. And for reliability analysis, 60 normal fetuses were randomly selected to undergo two consecutive measurements within a 10-min interval, and the images were saved for analysis offline. Measurements of biometric sizes were performed on fetuses by two independent examiners (Jinrong Liu and Min Hou), who were blind to each other's measurements. Intraclass and interclass correlation coefficients (ICCs) were used to compare the reliability of each index.

For clinical application, an additional 28 fetuses of singleton pregnancies with suspected abnormal posterior fossa contents based on prenatal ultrasonographic findings were assessed according to the classification and diagnostic methods [13]. We screened these including Dandy–Walker malformation (DWM), vermian hypoplasia (VH), Blake's pouch cyst (BPC), and mega cisterna magna (CM) using the above method to evaluate if the established criteria and minute structure findings were helpful in clinical diagnosis.

Data acquisition and measurement

After routine screenings, we used a combination of qualitative findings of the minute structure (visualization of fastigium and fissures) as well as biometry to evaluate the cerebellar vermis. Once the sagittal view was obtained, with a good display of the corpus callosum, thalamus, tentorium, and cerebellar vermis, the volume scan procedure was activated with a volume sweep angle of 65°, using previous studies as a Ref. [2, 11]. An offline analysis was performed with 4D View software (GE Healthcare, Kretz Ultrasound). Visualization of the mid-sagittal plane structure was preferably performed by static volume contrast imaging (VCI) with the slice thickness set to 1.9–2.1 mm. When images of fetal cerebellar vermis lobules and fissures on the mid-sagittal plane were obtained, biometric sizes were measured, including the anterior–posterior length (AP) (distance between the central lobule and the tuber vermis), cranio-caudal length (CC) (distance between the culmen and the uvula), circumference (C), and surface area (SA) (Fig. 1). All measurements were performed three times to get an average value.

Statistical analysis

Statistical analysis was completed using SPSS software, Version 20.0 (IBM Corporation, Somers, NY). Data were expressed as the mean plus or minus two standard deviations. *Z*-score conversions were made for each fetus to compare biometric values independently of GA; normal values were plotted to GA to establish a nomogram. Linear regression analysis was utilized to obtain the best fit for the normal range in the period from 16 to 41 weeks. Mann–Whitney *U* test analysis was used to compare the values in the case and control groups. Intra- and inter-observer reproducibility were assessed by ICC. $P < 0.05$ was considered statistically significant.

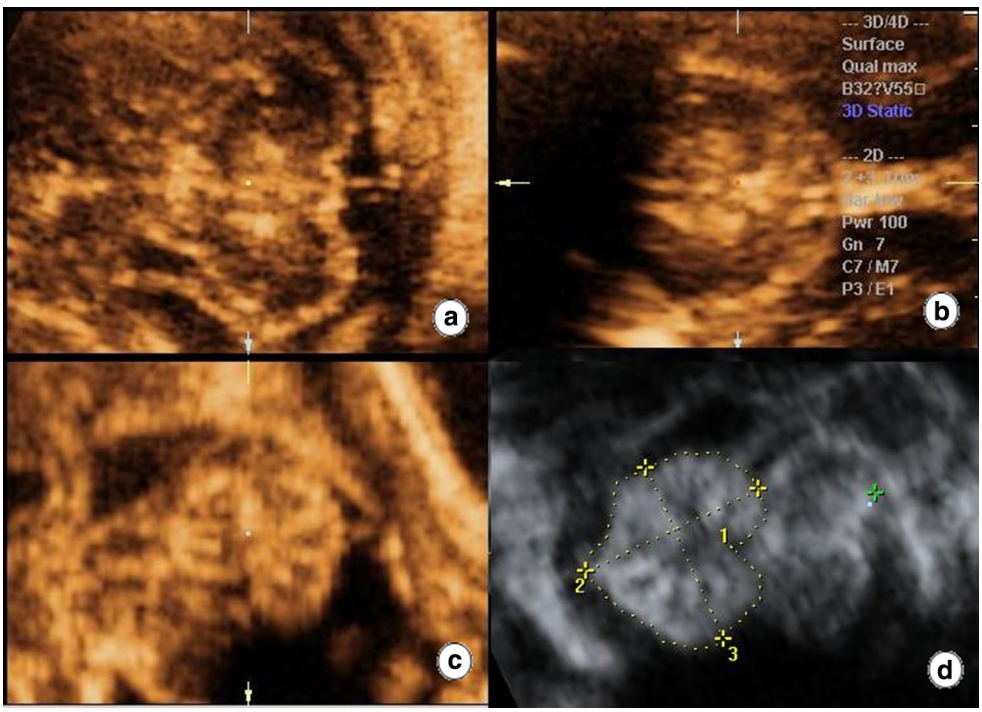

Fig. 1 Images and measurement of the normal fetal cerebellar vermis by 3D US. **a**–**c** Three mutually perpendicular planes (planes A, B and C). **d** Circumference and surface area (cursor 1), antero-posterior length (cursor 2), and cranio-caudal length (cursor 3)

Results

Normal fetuses

Measurements were acquired in 438 normal singleton fetuses with GA between 16 and 41 weeks (mean GA 26.8 weeks ± 1.9 weeks).

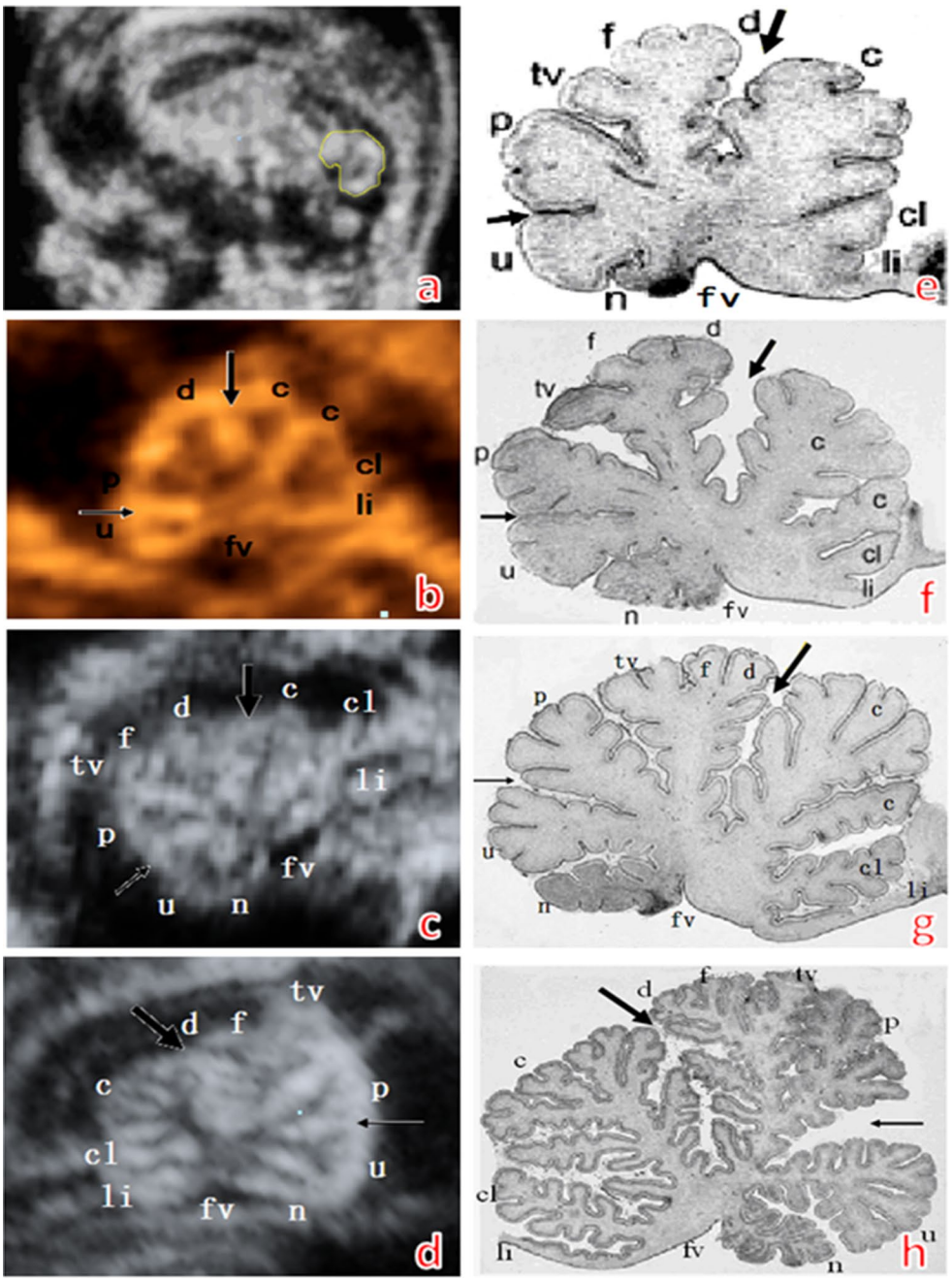

Fig. 2 A comparison between normal cerebellar vermis images obtained on the mid-sagittal plane by 3D US and autopsy. **a**–**d** are mid-sagittal views of the fetal cerebellar vermis at 19, 22, 25, and 28 weeks GA, respectively; **e**–**h** represent pathological sections of the cerebellar vermis at the same age (cited from Kapur et al. *Birth Defects Research (Part A), 2009;* this material is reproduced with the permission of John Wiley & Sons, Inc.). The fastigial recess of the fourth ventricle (open triangle), primary fissure (thick arrow), and secondary fissure (thin arrow)

Minute structures on mid-sagittal plane

The fissures between lobules were hyperechoic and the intralobule parts were hypoechoic. Cerebellar vermis contours and the fastigial recess of the fourth ventricle were visible around Week 19 (Fig. 2a). As embryonic development of the cerebellar vermis progressed, the main lobules and fissures, the primary fissure, and the fastigial recess of the fourth ventricle were visible by Week 22, but the image boundary of the central lobule, lingula, folium vermis, and nodulus were indistinguishable at this time (Fig. 2b). All nine lobules could be grossly distinguished at Week 25 (Fig. 2c), and arborization of the lobules continued throughout the vermis until Week 28, when all nine lobules, fissures, and the fourth ventricle were clearly displayed, and even the subtle arborization of some lobules could be seen (Fig. 2D).

Biometric size data

The development of the cerebellar vermis structure essentially followed the embryonic development process. Biometric sizes increased with GA, and there was a significant correlation between the values of fetal AP, CC, C, SA, and GA ($R^2 = 0.925$, 0.923, 0.967, and 0.958, respectively; all $P < 0.05$). The regression formulae were: Ln (AP) = − 11.013 + (1.229 × GA) + (− 0.008 × $GA^{2)}$; Ln (CC) = − 11.034 + (1.217 × GA) + (− 0.026 × GA^2); Ln (C) = − 39.421 + (4.289 × GA) + (− 0.026 × GA^2); Ln (SA) = − 0.569 + (− 0.005 × GA) + (0.004 × GA^2).

Intra- and inter-observer reproducibility

Each index for cerebellar vermis measurement by 3D US was good to various degrees in terms of intra- and inter-observer consistency and repeatability. The ICCs are shown in Table 1.

Fetuses with cerebellar vermis malformations

A total of 28 fetuses suspected of having abnormal posterior fossa contents (DWM, $n = 4$; VH, $n = 9$; BPC, $n = 5$, and CM, $n = 10$) were included in the study with a mean GA of 29.3 ± 2.3 weeks, depending on prenatal ultrasonographic findings. Among these, three (11%) cases were lost to follow-up because autopsy reports were not available or could not otherwise be obtained. Of the remaining 25 cases, there were associated malformations in 10 (40%) cases, including other central nervous system abnormalities and cardiac abnormalities. Combining observation of the fetal cerebellar vermis minute structure with quantitative evaluation of cerebellar vermis development on the mid-sagittal plane, the prenatal diagnosis was confirmed postnatally or at autopsy in 88% of cases. Ten fetuses were terminated during pregnancy and underwent autopsy. Prenatal ultrasonographic results from all four fetuses in the DWM group and five fetuses in the VH group were consistent with the autopsy reports. On ultrasound follow-up, intrauterine regression of the abnormal posterior fossa findings throughout gestation was noted in ten cases: the cyst disappeared in two of the four cases in the BPC group, with the vermis returning to its normal

Table 1 The ICCs for intra- and inter-observer reproducibility by 3D US

Group	SA ICC (95% CI)	C ICC (95% CI)	AP ICC (95% CI)	CC ICC (95% CI)
Interclass by 3DUS	0.992 0.984–0.996	0.986 0.975–0.993	0.969 0.942–0.984	0.982 0.965–0.990
Intraclass by 3DUS	0.989 0.980–0.994	0.970 0.943–0.984	0.961 0.927–0.979	0.954 0.915–0.975

CV cerebellar vermis, *ICC* interclass correlation coefficient, *CI* confidence interval, *AP* antero-posterior length, *CC* cranio-caudal length, *C* circumference, *SA* surface area

Table 2 Sonography in fetuses with cerebellar vermis malformations, associations with other anomalies, intrauterine regression, outcome and accuracy of prenatal diagnosis

Prenatal sonographic diagnosis	Total cases (*n*)	Cases with associated anomalies (*n*)	Lost to follow-up	Terminations of pregnancy	Regression in utero (*n*)	Sonographic diagnosis confirmed (*n* %)
DWM	4	4	0	4	0	4/4 = 100%
VH	9	5	2	6	0	5/7 = 71.42%
BPC	5	1	1	0	2	3/4 = 75%
CM	10	0	0	0	9	10/10 = 100%
Total (*n*)	28	10	3	10	11	22/25 = 88%

position, reaching term of gestation (excluding one case that was lost to follow-up), likely due to late fenestration. The posterior fossas of the nine fetuses in the CM group were all less than 10 mm at term, and only one fetus was confirmed as intrauterine growth restriction (IUGR) by postpartum follow-up of the enlarged posterior fossa (prenatal 133 mm, postnatal 152 mm) at birth. At the time of manuscript preparation, no identifiable malformation could be found in the 14 fetuses in the BPC and CM groups (Table 2 lists the defects present in greater detail).

Minute structures on the mid-sagittal plane

In the DWM group, no recognizable cerebellar vermis structures were exhibited (marked or complete absence); the boundary of the lobules was blurred and the primary fissure and secondary fissure were not visible or were blurred. The cerebellar vermis showed moderately severe/severe malrotation. The fastigial recess of the fourth ventricle was deficient. In the VH group, arborization of the lobules was reduced throughout the cerebellar vermis and all lobules were simplified and lacked folia; the nodulus of the inferior vermis was elongated and became long and thin; the primary fissure and secondary fissure were either partially invisible or completely invisible. The cerebellar vermis showed moderate/moderately severe malrotation. The fastigial recess of the fourth ventricle was shallow and relatively flat (Fig. 3). In the BPC group, arborization of the lobules was pronounced throughout the cerebellar vermis compared to normal fetuses of the same GA. The cerebellar vermis showed mild/moderate malrotation. The fastigial recess of the fourth ventricle and the upper wall of the cyst were clearly visible. In the CM group, arborization of the main lobules occurred throughout the cerebellar vermis; the primary fissure and the fastigial recess of the fourth ventricle were clearly visible and no other relevant central nervous system abnormalities were found.

Biometric data

The biometric data are shown in Table 3. The SA values of the cerebellar vermis in the DWM group were significantly reduced (absence $< (\bar{x} - 2SD)$ and more than 50% compared to normal at the same GA), and the SA values of the VH group were reduced (absence $< (\bar{x} - 2SD)$ but less than 50%). The BPC and CM groups were nearly normal in gross proportions, except for the IUGR case with a reduced SA (Fig. 4).

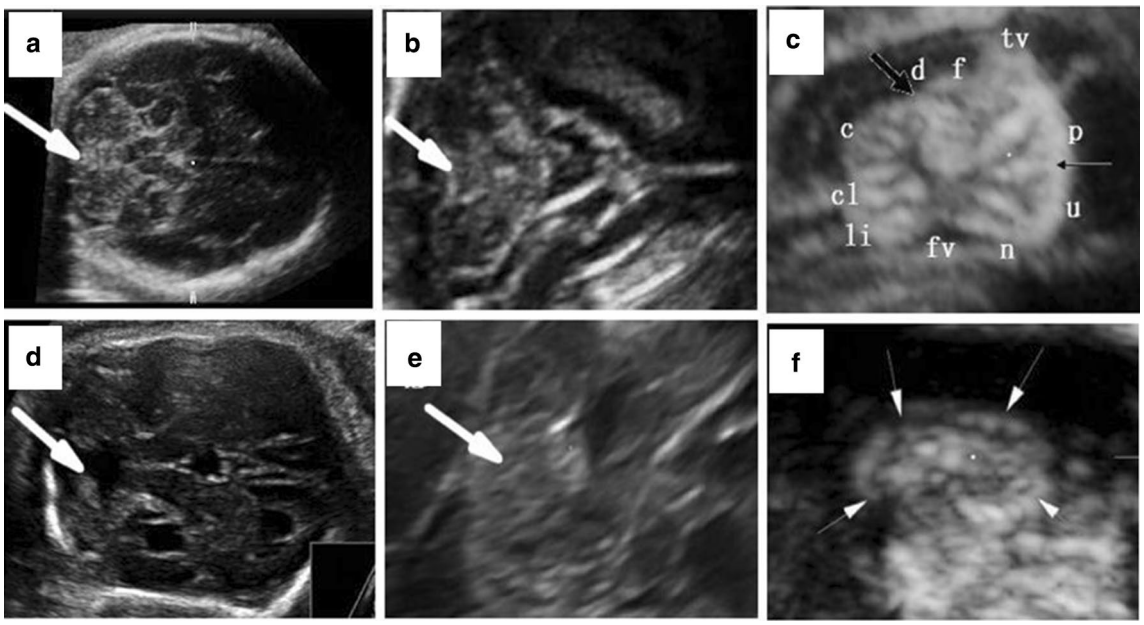

Fig. 3 Images of the cerebellar vermis at 28 weeks gestational age. Images of a normal fetus: images of the fetal cerebellar vermis displayed clearly on **a** the transverse plane and **b** the coronal plane; **c** image on the mid-sagittal plane of the SA of a normal fetus, with all nine lobules and fissures seen clearly. Primary fissure (thick arrow) and secondary fissure (thin arrow). In comparison, images of the cerebellar vermis on **d** the transverse plane and **e** coronal plane are vague in a VH fetus. **f** On the mid-sagittal plane of a VH fetus, the SA is smaller in contrast to a normal fetus at the same GA, and at the boundary, the cerebellar vermis is blurred (arrow) and the lobules are less arborized. *SA* surface area, *GA* gestational age, *c* culmen, *cl* central lobule, *d* declive, *f* folium vermis, *li* lingula, *n* nodulus, *p* pyramis, *tv* tuber vermis, *u* uvula

Table 3 Visualization of cerebellar vermis malformations ($n=28$)

Case	GA (weeks)	AP (mm)	CC (mm)	C (mm)	SA (cm^2)	*Z*-Score of SA
DWM						
1	26	0	0	0	0	−8.95*
2	28	7.9	8.1	25.3	0.48	−9.40*
3	29	11.2	12.7	41.8	0.91	−6.56*
4	30	0	0	0	0	−9.43*
VH						
1	23	10.3	10.6	33.6	0.76	−3.40*
2	24	8.8	8.2	34.7	0.71	−4.60*
3	29	16.4	16.9	54.4	1.71	−3.36*
4	30	18.2	15.5	56.7	1.99	−2.80*
5	31	20.3	18.2	64.7	2.48	−1.93*
6	31	18.6	19.3	60.5	2.37	−2.33*
7	32	16.1	19.2	60.3	2.23	−4.21*
8	32	15.1	17.2	55.6	2.01	−5.13*
9	40	21.8	23.8	76.4	3.51	−3.73*
BPC						
1	21	10.8	10.9	38.1	0.71	−1.79
2	26	14.2	15.1	50.1	1.45	−1.32
3	32	24.3	23.5	74.9	3.37	0.54
4	32	22.8	24.1	76.1	3.65	1.58
5	35	21.8	24.7	78.1	3.61	−0.07
CM						
1	24	13.3	13.9	48.2	1.43	0.20
2	25	14.1	14.7	50.7	1.58	0.06
3	28	17.7	18.2	61.5	2.41	0.25
4	29	20.6	20.6	67.0	2.82	1.08
5	30	15.2	17.2	56.1	2.07	−2.53*
6	30	16.5	20.9	66.2	2.61	0.73
7	30	19.2	19.9	69.1	2.95	0.40
8	31	17.2	20.2	68.2	2.61	−1.44
9	32	22.0	23.1	72.0	3.38	0.58
10	33	19.6	23.4	72.6	3.30	−0.04

SA on mid-sagittal plane $< \bar{x} - 2$SD at the same GA control group (*). *CV* cerebellar vermis, *SA* surface area, *GA* gestational age, *AP* antero-posterior length, *CC* cranio-caudal length, *C* circumference, *SA* surface area

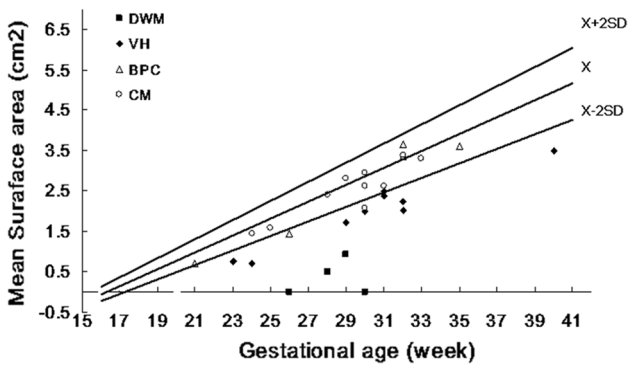

Fig. 4 Surface area comparison between DWM, VH, BPC, CM, and control groups at different gestational ages

Discussion

In our study, 438 fetuses were evaluated for the minute structure of the fetal cerebellar vermis at different GAs. Using our 3D US multiplanar approach, prenatal diagnosis of cerebellar vermis malformations was correct in almost 90% of cases. The main structure of the cerebellar vermis could be visualized at Week 19, which is earlier than shown in previous studies [14, 15]. With high reproducibility, measurements were effective in clinical practice.

Several papers have reported the reference indices for fetal vermis measurement and assessment of fetal posterior fossa anomalies [16, 17]. Our study added to their findings by observing fine structures and identifying the location of each gauge line. And an interesting finding of our study was

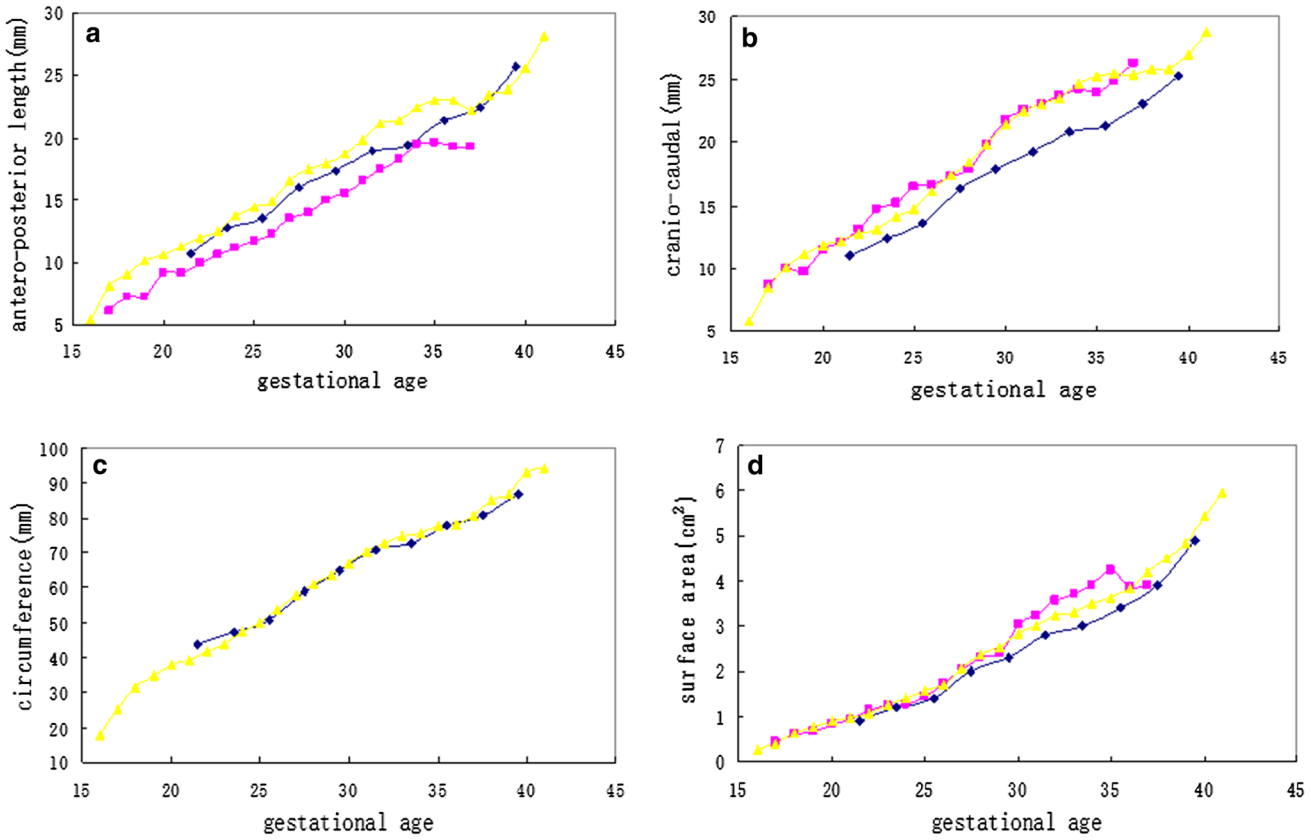

Fig. 5 Comparison chart of fetal cerebellar vermis biometric data according to gestational age. **a** Purple, blue, and yellow lines represent the AP data from Xie HN et al., Malinger et al., and our study, respectively. **b** Purple, blue, and yellow lines represent the CC data from Xie HN et al., Malinger et al., and our study, respectively. **c** Blue and yellow lines represent the C data from Malinger et al. and our study, respectively. **d** Purple, blue, and yellow lines represent the SA data from Xie HN et al., Malinger et al., and our study, respectively

that the variability in AP and CC values was large compared to that in previous studies, while SA and C values were comparable [15, 18] (Fig. 5). That indicated the precision and instability of cerebellar vermis abnormality evaluation based on SA and C detection. This could have resulted from the different method they used (transvaginal inspection [15]) and the nuance of starting/ending points in their measurements. In other words, it is necessary to identify the insertion of each gauge line based on the subtle structure imaged.

In our study, a communication of the fourth ventricle with the posterior cranial fossa was found in one of the VH cases. The closure of the cerebellar vermis was delayed until 28 weeks of GA and eventually returned to normal after postnatal evaluation. This delayed closure of the cerebellar vermis was evidenced by both sonographic studies [19] and magnetic resonance studies [20]. As Brennan et al. [19] reported, the cerebellar vermis was complete after Week 18–20, but studies conducted by Zalel et al. [21] and Malinger et al. [15] found that closure of the cerebellar vermis of some fetuses was delayed until Week 20, or even as late as Week 27, and eventually returned to normal. That might explain the poor correlation between prenatal ultrasound findings and postnatal follow-up (autopsy or radiologic imaging) to some degree. In addition, delayed rotation of the cerebellar vermis could also contribute to the diagnosis of inferior vermian hypoplasia [22]. Another point to note was that the excessive tilt of the transcranial fossa section (C plane) during ultrasound examination resulted in the false appearance of posterior fossa cistern widening and communication with the fourth ventricle [23]. In general, caution is warranted in diagnosing cerebellar anomalies too early because of the incomplete development of the vermis, and instead, all fetuses should be followed until Week 27–28 or until delivery or postpartum, especially in suspected BPC and CM fetuses.

Among the cerebellar vermis biomarkers, we recommended SA on the mid-sagittal plane as a primary indicator to assess cerebellar vermis deformity, which was similar to previous studies [14]. First, as we found, the SA decreased at least 50% in the DWM group, and the SA in the VH group decreased during $\bar{x} - 2SD$ to 50%. That would be an easy but important clue to distinguish DWM cases from VH cases.

Table 4 The diagnostic criteria for each cerebellar vermis abnormality in our study

	DWM	VH	BPC	CM
Surface area of vermis	≤ 50%	50% < SA <	Normal size	Normal size
Rotation Malrotation of vermis	Moderately severe/severe	Moderate/moderately severe	Mild/moderate	Normal
Roof of the 4th ventricle	Deficiency	Shallow and relatively flat	Visualization of BPC roof	Normal
Cisterna magna	Communication with the 4th ventricle	Communication with the 4th ventricle	Normal or enlarged	Enlarged
Minute structure	1. No recognizable cerebellar vermis structures was shown 2. The primary/secondary fissures and lobules were absent or blurred	1. The vermis not full; the inferior vermis was elongated 2. The primary/secondary fissures were absent or partly absent; arborization of the lobules reduced	1. Normomorph 2. Arborization of the lobules existed	1. Normomorph 2. Arborization of the lobules existed 3. No other relevant central nervous system abnormalities

DWM Dandy–Walker malformation, *VH* vermis hypoplasia, *BPC* Blake's pouch cyst, *CM* mega cisterna magna

Table 5 The ICCs for intra- and inter-observer reliability of cerebellar vermis by 3D US

Suggested cut-off value		ICC in present study							
		Intra-observer				Inter-observer			
ICC	Reliability	SA	C	AP	CC	SA	C	AP	CC
< 0.95	Very poor								
0.95–0.98	Poor		0.970	0.961	0.954			0.969	
0.98–0.99	Moderate	0.989					0.986		0.982
0.99–0.998	Good					0.992			
> 0.998	Very good								

ICC interclass correlation coefficient, *AP* antero-posterior length, *CC* cranio-caudal length, *C* circumference, *SA* surface area

The diagnostic criteria for each cerebellar vermis abnormality in our study are summarized in Table 4. These criteria were a slightly expanded version of those proposed previously, combined with data regarding the minute structures observed in our study. Second, as indicated above, SA and C detection was more precise and stable than AP and CC detection in cerebellar vermis abnormality evaluation. Last but not least, taking reliability into consideration, SA was excellent in terms of reliability, consistent with those in both ultrasound and MR studies [2, 7]. And SA was superior to other biomarkers in both interclass and intraclass detection according to the cut-off values published by Martins and Nastri [24] (shown in Table 5). Therefore, we deemed SA was an optimal reference for diagnosis and antidiastole of cerebellar vermis abnormalities, which is worth highlighting in the context.

At this juncture, we have to mention that in our study, SA of the IURG fetus in the CM group was small after birth and returned to normal after 10 months of postpartum follow-up. There is no exact explanation for this phenomenon, but we speculated that this might be related to cerebellar vermis postnatal catch-up growth caused by IUGR. On the other hand, combining with the development of minute structures was indispensable in the cerebellar vermis malformation evaluation.

Conclusion

In conclusion, we have described the cerebellar vermis minute structure on the mid-sagittal plane using 3D US in various embryonic stages. In addition, we have proposed minute structure criteria to diagnose and differentiate cerebellar vermis malformations. Finally, we propose that SA could be a superior indicator to assess cerebellar vermis malformations. Further fetal series are needed to confirm the conclusions reached in this study.

Acknowledgements We thank all the project participants for their contributions and Medjaden Bioscience Limited for assisting in the preparation of this manuscript.

Funding This study was supported by Grants from the National Natural Science Foundation of China (no. 81271587) and the Key Program of Scientific Research of Fujian Medical University, P. R. China (no.

09ZD015) and the Natural Science Foundation of Fujian Province (no. 2015D015 & no. 2015J01363).

Compliance with ethical standards

Informed consent Informed consent was obtained from patients and healthy controls in this study, and the study was approved by the Ethics Committee of the School of Medicine, Xiamen University.

Conflict of interest The authors declare that they have no conflicts of interest.

References

1. Dudek K, Nowakowska-Kotas M, Kędzia A. Mathematical models of human cerebellar development in the fetal period. J Anat. 2018;232:596–603.
2. Katorza E, Bertucci E, Perlman S, et al. Development of the fetal vermis: new biometry reference data and comparison of 3 diagnostic modalities-3d ultrasound, 2d ultrasound, and mr imaging. AJNR Am J Neuroradiol. 2016;37:1359–66.
3. Wüest A, Surbek D, Wiest R, et al. Enlarged posterior fossa on prenatal imaging: differential diagnosis, associated anomalies and postnatal outcome. Acta Obstet Gynecol Scand. 2017;96:837–43.
4. D'Antonio F, Khalil A, Garel C, et al. Systematic review and meta-analysis of isolated posterior fossa malformations on prenatal ultrasound imaging (part 1): nomenclature, diagnostic accuracy and associated anomalies. Ultrasound Obstet Gynecol. 2016;47:690–7.
5. Kapur RP, Mahony BS, Finch L, et al. Normal and abnormal anatomy of the cerebellar vermis in midgestational human fetuses. Birth Defects Res A Clin Mol Teratol. 2009;85:700–9.
6. Dovjak GO, Brugger PC, Gruber GM, et al. Prenatal assessment of cerebellar vermian lobulation: fetal MRI with 3 Tesla postmortem correlation. Ultrasound Obstet Gynecol. 2017. https://doi.org/10.1002/uog.18826.
7. Zhao D, Cai A, Zhang J, et al. Measurement of normal fetal cerebellar vermis at 24–32 weeks of gestation by transabdominal ultrasound and magnetic resonance imaging: a prospective comparative study. Eur J Radiol. 2018;100:30–5.
8. Chapman T, Mahalingam S, Ishak GE, et al. Diagnostic imaging of posterior fossa anomalies in the fetus and neonate: part 2, posterior fossa disorders. Clin Imaging. 2015;39:167–75.
9. Rizzo G, Pietrolucci ME, Mammarella S, et al. Assessment of cerebellar vermis biometry at 18–32 weeks of gestation by three-dimensional ultrasound examination. J Matern Fetal Neonatal Med. 2012;25:519–22.
10. You JH, Lv GR, Liu XL, et al. Reference ranges of fetal spleen biometric parameters and volume assessed by three-dimensional ultrasound and their applicability in spleen malformations. Prenat Diagn. 2014;34:1189–97.
11. Frisova V, Srutova M, Hyett J. 3-D volume assessment of the corpus callosum and cerebellar vermis using various volume acquisition and post-processing protocols. Fetal Diagn Ther. 2018;43:199–207.
12. Rizzo G, Abuhamad AZ, Benacerraf BR, et al. Collaborative study on 3-dimensional sonography for the prenatal diagnosis of central nervous system defects. J Ultrasound Med. 2011;30:1003–8.
13. Chapman T, Mahalingam S, Ishak GE, et al. Diagnostic imaging of posterior fossa anomalies in the fetus and neonate: part 1, normal anatomy and classification of anomalies. Clin Imaging. 2015;39:1–8.
14. Zalel Y, Yagel S, Achiron R, et al. Three-dimensional ultrasonography of the fetal vermis at 18 to 26 weeks' gestation: time of appearance of the primary fissure. J Ultrasound Med. 2009;28:1–8.
15. Malinger G, Ginath S, Lerman-Sagie T, et al. The fetal cerebellar vermis: normal development as shown by transvaginal ultrasound. Prenat Diagn. 2001;21:687–92.
16. Cignini P, Giorlandino M, Brutti P. Reference charts for fetal cerebellar vermis height: a prospective cross-sectional study of 10605 fetuses. PLoS One. 2016;11:e0147528.
17. Spinelli M, Sica C, Meglio LD, et al. Fetal cerebellar vermis circumference measured by 2-dimensional ultrasound scan: reference range, feasibility and reproducibility. Ultrasound Int Open. 2016;2:E124–8.
18. Xie Hongning CD, Zhu Yunxiao LL. Study on the development of fetal cerebellar vermis with the third plane image of three-dimensional ultrasonography. Chin J Pract Gynecol Obstet. 2006;22:32–4.
19. Bromley B, Nadel AS, Pauker S, et al. Closure of the cerebellar vermis: evaluation with second trimester US. Radiology. 1994;193:761–3.
20. Babcook CJ, Chong BW, Salamat MS, et al. Sonographic anatomy of the developing cerebellum: normal embryology can resemble pathology. AJR Am J Roentgenol. 1996;166:427–33.
21. Zalel Y, Gilboa Y, Gabis L, et al. Rotation of the vermis as a cause of enlarged cisterna magna on prenatal imaging. Ultrasound Obstet Gynecol. 2006;27:490–3.
22. Pinto J, Paladini D, Severino M, Morana G, Pais R, Martinetti C, Rossi A. Delayed rotation of the cerebellar vermis: a pitfall in early second-trimester fetal magnetic resonance imaging. Ultrasound Obstet Gynecol. 2016;48:121–4.
23. Paladini D, Volpe P. Posterior fossa and vermian morphometry in the characterization of fetal cerebellar abnormalities: a prospective three-dimensional ultrasound study. Ultrasound Obstet Gynecol. 2006;27:482–9.
24. Martins WP, Nastri CO. Interpreting reproducibility results for ultrasound measurements. Ultrasound Obstet Gynecol. 2014;43:479–80.